China Ocean Eng., Vol. 26, No. 3, pp. 521 – 534

DOI 10.1007/s13344-012-0039-8, ISSN 0890-5487

Robust Leader-Follower Formation Tracking Control of Multiple Underactuated Surface Vessels*

PENG Zhou-hua (彭周华)[a], WANG Dan (王　丹)[a, 1],
LAN Wei-yao (兰维瑶)[b] and SUN Gang (孙　刚)[a]

[a] *Marine Engineering College, Dalian Maritime University, Dalian 116026, China*
[b] *Department of Automation, Xiamen University, Xiamen 361005, China*

(Received 1 April 2011; received revised form 14 December 2011; accepted 20 February 2012)

ABSTRACT

This paper is concerned with the formation control problem of multiple underactuated surface vessels moving in a leader-follower formation. The formation is achieved by the follower to track a virtual target defined relative to the leader. A robust adaptive target tracking law is proposed by using neural network and backstepping techniques. The advantage of the proposed control scheme is that the uncertain nonlinear dynamics caused by Coriolis/centripetal forces, nonlinear damping, unmodeled hydrodynamics and disturbances from the environment can be compensated by on line learning. Based on Lyapunov analysis, the proposed controller guarantees the tracking errors converge to a small neighborhood of the origin. Simulation results demonstrate the effectiveness of the control strategy.

Key words: *marine surface vessel*; *formation control*; *neural network*; *backstepping*; *leader-follower*

1. Introduction

The last decade has witnessed the widespread interest in formation control of multiple vehicles from control community. This is partially due to the fact that there is an increasing need for utilizing multiple vehicles to operate effectively as a team, where it contributes to enhanced efficiency, reduced system cost and increased robustness towards individual failures. Relevant applications arising in the marine industry include automatic ocean exploration, environmental monitoring, towing of large structures, surveillance of territorial waters, and so on. To achieve a desired formation, various control schemes have been proposed, which include leader-follower strategy (Wang, 1991), virtual structure method (Beard *et al*., 2001), behavioral approach (Balch and Arkin, 1999), and artificial potential function (Leonard and Fiorelli, 2001). Most studies investigating the formation control usually use one or more of these approaches in either a centralized or distributed manner.

Among these control schemes mentioned above, the leader-follower strategy seems to be much preferred due to its simplicity and scalability. During the past decade, the marine control community has focused on the formation control. Most of works appeared to have been done within the leader-follower framework. The leader-follower formation control involves the control of each vehicle

* This work was financially supported by the National Natural Science Foundation of China (Grant Nos. 60674037, 61074017 and 61074004), the Program for New Century Excellent Talents in Universities (Grant No. NCET-09-0674), and the Program for Liaoning Excellent Talents in Universities (Grant No. 2009R06).
1 Corresponding author. E-mail: dwang@dlmu.edu.cn

to follow a predefined path, which can be seen in the references (Skjetne *et al*., 2002; Børhaug *et al*., 2006; Ihle *et al*., 2006; Aguiar *et al*., 2006; Almeida *et al*., 2007), or to track a desired location relative to a reference point (Fahimi, 2006; Breivik *et al*., 2008b; Cui *et al*., 2010). As a consequence, the coordinated path following and coordinated target tracking problems have attracted great attention (Aguiar *et al*., 2009; Breivik, 2010). As for the coordinated path following, a fleet of vehicles is required to track a series of pre-defined spatial paths, while holding a desired formation pattern at a desired speed (Aguiar *et al*., 2009). Skjetne *et al*. (2002) studied the coordinated path following problem of marine craft, where vectorial backstepping is used to solve the geometric task and dynamic task. Ihle *et al*. (2006) studied the synchronized path following problem of marine craft, where the individual systems are controlled by a path-following design and the path variables are synchronized by using a passivity-based synchronization algorithm. Aguiar *et al*. (2006) studied the cooperative path following of underwater vehicles, where the Lyapunov-based technique and graph theory are brought together to yield a decentralized formation control structure. Almeida *et al*. (2007) studied the coordinated path following problem of multiple vehicles with discrete periodic communication. In the coordinated path following, however, the formation heavily depends on the priori knowledge of the predefined path. Once the mission is changed and something unexpected happens, the path must be redesigned. As an alternative, the target tracking scheme seems to offer greater flexibility and scalability over the path following by defining some virtual points for the followers to track. Breivik *et al*. (2008b) considered the straight line target tracking problem of unmanned surface vehicles. The motion control system employs a guidance principle originally developed for intercepting missiles, as well as a novel velocity controller inspired by maneuverability and agility concepts found in fighter aircraft literature. Cui *et al*. (2010) studied the leader-follower target tracking problem of underactuated autonomous underwater vehicle, where a virtual vehicle is constructed such that its trajectory converges to the reference point. Based on backstepping synthesis, an adaptive position tracking law is designed for the follower to track the virtual vehicle.

It is noticed that most studies aforementioned above typically used some variants of the model by Fossen (2002), assuming that the model parameters are either perfectly known or known with a small degree of uncertainty (Skjetne *et al*., 2002; Ihle *et al*., 2006; Almeida *et al*., 2007). In practice, it is quite difficult to obtain the model parameter accurately, especially with regard to the hydrodynamic damping matrix. The presence of the modeling errors, in the form of parametric and function uncertainties, unmodeled hydrodynamic and disturbances from the environment, is a common problem. Neural network (NN) as one of the universal approximators has been demonstrated very useful to handle the uncertain dynamics in several studies (Polycarpou, 1996; Lewis *et al*., 1996; Zhang *et al*., 1999; Hovakimyan *et al*., 2002; Wang and Huang, 2002, 2005; Wang, 2010; Chen *et al*., 2010). The rigorous proofs of convergence, stability and performance can be found in Polycarpou (1996) and Lewis *et al*. (1996), which are well known. NNs are introduced to deal with the uncertain dynamics in formation control system and can be found in Chen and Li (2008), Dierks and Jagannathan (2010), Cui *et al*. (2010), and Peng *et al*. (2011a and 2011b). However, neural adaptive control has not been fully explored for the control of marine surface vessel. The trajectory tracking problem for fully-actuated ocean vessel is considered in Tee and Ge (2007), where radial basic function (RBF) NN is employed to handle both unknown uncertainties and time-varying disturbance. The focus of this research, however, is on the formation control of multiple underactuated vessels rather than the trajectory tracking control for fully-actuated vehicle as in Tee and Ge (2007).

In this paper, we consider the leader-follower formation control problem of underactuated surface vessels (USV) in the presence of unknown nonlinear dynamics and disturbances from the environment. Motivated by the pure pursuit guidance developed for intercepting missiles described in Breivik *et al.* (2008a) and the control development for the point-to-point navigation of underactuated ships in Li *et al.* (2008), a pure-pursuit target tracking control scheme is proposed to achieve a leader-follower formation. The formation is performed by the follower to intercept a virtual target defined relative to the leader. The robust adaptive formation tracking law is developed by utilizing neural network and backstepping techniques. Compared with the existing results, the proposed control law takes the following advantages: first, the proposed controller is universal and model-independent, while the formation controllers in Skjetne *et al.* (2002), Ihle *et al.* (2006), Almeida *et al.* (2007), and Breivik *et al.* (2008a) depend on the accurate model of the vessel, which is unavailable in practice; second, the nonlinear dynamics caused by Coriolis/centripetal force, nonlinear damping, unmodeled hydrodynamics and disturbances from the environment can be compensated by on line learning; third, the developed control law avoids the singularity problem appearing in Li *et al.* (2008). In addition, the linear-in-parameters assumption in the study is also removed.

This paper is organized as follows: Section 2 introduces the problem formulation and summarizes some preliminaries. Section 3 presents the formation tracking control design. Section 4 gives the simulation results. Section 5 concludes this paper.

2. Problem Formulation and Preliminaries

2.1 Vessel Model

Consider a group of N USVs, each of which is governed by following dynamics found in Fossen (2002) with kinematics

$$\dot{\boldsymbol{\eta}}_i = \boldsymbol{J}(\psi_i)\boldsymbol{v}_i, \tag{1}$$

and kinetics

$$\boldsymbol{M}_i\dot{\boldsymbol{v}}_i + \boldsymbol{C}_i(\boldsymbol{v}_i)\boldsymbol{v}_i + \boldsymbol{D}_i(\boldsymbol{v}_i)\boldsymbol{v}_i + \boldsymbol{\varDelta}_i(\boldsymbol{v}_i, \boldsymbol{\eta}_i) = \boldsymbol{\tau}_i + \boldsymbol{w}_i(t), \tag{2}$$

where

$$\boldsymbol{J} = \begin{bmatrix} \cos\psi_i & -\sin\psi_i & 0 \\ \sin\psi_i & \cos\psi_i & 0 \\ 0 & 0 & 1 \end{bmatrix}; \quad \boldsymbol{M}_i = \begin{bmatrix} m_{11i} & 0 & 0 \\ 0 & m_{22i} & m_{23i} \\ 0 & m_{32i} & m_{33i} \end{bmatrix}; \quad \boldsymbol{\varDelta}_i = \begin{bmatrix} \varDelta_u(\nu_i, \eta_i) \\ \varDelta_\upsilon(\nu_i, \eta_i) \\ \varDelta_r(\nu_i, \eta_i) \end{bmatrix};$$

$$\boldsymbol{C}_i = \begin{bmatrix} 0 & 0 & c_{13i}(\nu_i) \\ 0 & 0 & c_{23i}(\nu_i) \\ c_{31i}(\nu_i) & c_{32i}(\nu_i) & 0 \end{bmatrix}; \quad \boldsymbol{D}_i = \begin{bmatrix} d_{11i}(\nu_i) & 0 & 0 \\ 0 & d_{22i}(\nu_i) & d_{23i}(\nu_i) \\ 0 & d_{32i}(\nu_i) & d_{33i}(\nu_i) \end{bmatrix}.$$

$\boldsymbol{\eta}_i = [x_i, y_i, \psi_i]^{\mathrm{T}} \in \Re^3$ is the position and heading in the earth-fixed reference frame;

$\boldsymbol{v}_i = [u_i, \upsilon_i, r_i]^{\mathrm{T}} \in \Re^3$ is the velocity vector in the body-fixed reference frame; $\boldsymbol{\tau}_i = [\tau_{iu}, 0, \tau_{ir}]^{\mathrm{T}} \in \Re^3$ is the control input vector with τ_{iu} (the surge force) and τ_{ir} (the yaw moment); $\boldsymbol{w}_i = [w_{iu}, w_{i\upsilon}, w_{ir}]^{\mathrm{T}} \in \Re^3$ a vector of the time-varying disturbances induced by wind, wave and ocean current. $\boldsymbol{\Delta}_i(\boldsymbol{v}_i, \boldsymbol{\eta}_i) \in \Re^3$ denotes the unmodeled hydrodynamics; $\boldsymbol{M}_i \in \Re^{3\times3}$, $\boldsymbol{C}_i(\boldsymbol{v}) \in \Re^{3\times3}$, and $\boldsymbol{D}_i(\boldsymbol{v}_i) \in \Re^{3\times3}$ denote the inertia matrix, Coriolis/centripetal matrix, hydrodynamic damping matrix, respectively;

By choosing appropriate body-fixed frame origin as in Do and Pan (2006), the vehicle dynamics in Eqs. (1) and (2) can be written as:

$$\dot{x}_i = u_i \cos(\psi_i) - \upsilon_i \sin(\psi_i)\,; \tag{3}$$

$$\dot{y}_i = u_i \sin(\psi_i) + \upsilon_i \cos(\psi_i)\,; \tag{4}$$

$$\dot{\psi}_i = r_i\,; \tag{5}$$

$$\dot{u}_i = m_{11i}^{-1}\left[-c_{13i}(\nu_i)r_i - d_{11i}(\nu_i)u_i - \Delta_u(\nu_i,\eta_i) + w_{iu}(t) + \tau_{iu}\right]; \tag{6}$$

$$\dot{\upsilon}_i = m_{22i}^{-1}\left[-c_{23i}(\nu_i)r_i - d_{22i}(\nu_i)\upsilon_i - d_{23i}(\nu_i)r_i - \Delta_\upsilon(\nu_i,\eta_i) + w_{i\upsilon}(t)\right]; \tag{7}$$

$$\begin{aligned}\dot{r}_i = {} & m_{33i}^{-1}m_{32i}m_{22i}^{-1}\left[-c_{23i}(\nu_i)r_i - d_{22i}(\nu_i)\upsilon_i - d_{23i}(\nu_i)r_i - \Delta_\upsilon(\nu_i,\eta_i) + w_{i\upsilon}(t)\right] \\ & + m_{33i}^{-1}\left[-c_{31i}(\nu_i)u_i - c_{32i}(\nu_i)\upsilon_i - d_{32i}(\nu_i)\upsilon_i - d_{33i}(\nu_i)r_i - \Delta_r(\nu_i,\eta_i) + w_{ir}(t) + \tau_{ir}\right].\end{aligned} \tag{8}$$

2.2 Target Tracking

Let $\boldsymbol{q}_d(s_d) \in \Re^2$ be the position of the leader and $\boldsymbol{q}_{id} := [x_{id}, y_{id}]^{\mathrm{T}} \in \Re^2$ be the position of the virtual target. Then, the position of the virtual target can be calculated as:

$$\begin{aligned}&\boldsymbol{q}_{id} = \boldsymbol{q}_d(s_d) + \boldsymbol{R}(\psi_s)\boldsymbol{l}_i \\ &\boldsymbol{R}(\psi_s) = \begin{bmatrix}\cos(\psi_s) & -\sin(\psi_s) \\ \sin(\psi_s) & \cos(\psi_s)\end{bmatrix}\end{aligned} \tag{9}$$

where $\boldsymbol{l}_i \in \Re^2$ is a constant vector and $\boldsymbol{R}(\psi_s) \in \Re^{2\times2}$ is a transform matrix with ψ_s (the heading angle of the leader).

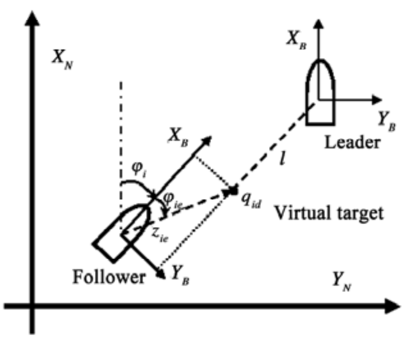

Fig. 1. Target tracking.

As illustrated in Fig. 1, to achieve the target-tracking of the virtual point q_{id}, define a distant tracking error:

$$z_{ie} = \sqrt{x_{ie}^2 + y_{ie}^2} \; ; \tag{10}$$

and a yaw tracking error:

$$\psi_{ie} = \psi_{id} - \psi_i \; ; \tag{11}$$

where $x_{ie} = x_{id} - x_i$, $y_{ie} = y_{id} - y_i$, $\psi_{id} = \arctan 2(y_{ie}, x_{ie})$; ψ_{id} denotes the desired angle of the follower relative to the target.

The control objective is to propose a control scheme for the *i*-th USV with dynamics in Eqs. (1) and (2), to intercept the virtual target q_{id} in Eq. (9), such that the tracking errors ψ_{ie} and z_{ie} in Eqs. (10) and (11) are guaranteed to be semi-globally uniformly ultimately bounded (SUUB).

2.3 Preliminaries

In the sequel, we will make use of universal approximation property of a feedforward NN to estimate the uncertain dynamics in Eq. (2). A single hidden layer (SHL) NN with x_k as the input and y_i the output is an input-output mapping defined as follows:

$$y_i = \sum_{r=1}^{N_2} \left\{ w_{ir} \sigma_r \left[\sum_{k=1}^{N_1} \vartheta_{rk} x_k + \vartheta_{r(N_1+1)} \right] \right\} + w_{i(N_2+1)}, \quad (i = 1, ..., N_3, r = 1, ..., N_2, k = 1, ..., N_1) , \tag{12}$$

where ϑ_{rk} is called the weight from the input neuron i to hidden neuron r ; $\vartheta_{r(N_1+1)}$ is the bias term of the hidden neuron r ; w_{ir} is the weight from the hidden neuron r to the output y_i ; $w_{i(N_2+1)}$ is the bias term to output y_i ; N_2 is the number of hidden neurons; σ_r is the activation function of the neuron. The common activation functions include sigmoid function and hyper-tangent function. For convenience, we will express the input-output mapping of NN as follows:

$$\boldsymbol{F}(x_1, ..., x_{N_1}) = \boldsymbol{W}^{\mathrm{T}} \boldsymbol{\sigma}(\boldsymbol{V}^{\mathrm{T}} \boldsymbol{\xi}) , \tag{13}$$

where $\boldsymbol{\xi} = [x_1, ..., x_{N_1}, 1]^{\mathrm{T}}$, $\boldsymbol{W}$ is a vector consisting of all w_{ir} , $\boldsymbol{\sigma} = [1, \sigma_1, ..., \sigma_{N_2}]$ is a vector consisting of all σ_r and $\boldsymbol{V}$ is a matrix with its *r*-th column given by $\boldsymbol{V}_r$, where $\boldsymbol{V}_r = [\vartheta_{1r}, ..., \vartheta_{N_1 r}, \vartheta_{(N_1+1)r}]^{\mathrm{T}}$.

The universal approximation theorem in Hornik (1991) claims that, given a continuous real-valued function $f : \boldsymbol{x} \to \Re^{N_3}$ with a compact set $\boldsymbol{x} \in \Re^{N_1}$, and for any $\varepsilon_M > 0$, there exist an ideal weight matrix $\boldsymbol{W}$ and ideal weight matrix $\boldsymbol{V}$ such that

$$f(x) = \boldsymbol{W}^{\mathrm{T}} \boldsymbol{\sigma}(\boldsymbol{V}^{\mathrm{T}} \boldsymbol{\xi}) + \boldsymbol{\varepsilon}(\boldsymbol{\xi}) , \tag{14}$$

where $\|\boldsymbol{\varepsilon}(\boldsymbol{\xi})\| \le \varepsilon_M$.

Let $\hat{\boldsymbol{W}}$ and $\hat{\boldsymbol{V}}$ be the estimates of the ideal weight $\boldsymbol{W}$ and $\boldsymbol{V}$; then, the estimation errors for the NN weights can be described as:

$$\tilde{\boldsymbol{W}} = \hat{\boldsymbol{W}} - \boldsymbol{W} \text{ and } \tilde{\boldsymbol{V}} = \hat{\boldsymbol{V}} - \boldsymbol{V} . \tag{15}$$

Let the hidden-layer output error for a given $\boldsymbol{\xi}$ be

$$\tilde{\boldsymbol{\sigma}} = \hat{\boldsymbol{\sigma}} - \boldsymbol{\sigma} = \boldsymbol{\sigma}(\hat{\boldsymbol{V}}^{\mathrm{T}}\boldsymbol{\xi}) - \boldsymbol{\sigma}(\boldsymbol{V}^{\mathrm{T}}\boldsymbol{\xi}). \tag{16}$$

Then, the function approximation error can be expressed by:

$$\hat{\boldsymbol{W}}^{\mathrm{T}}\boldsymbol{\sigma}(\hat{\boldsymbol{V}}^{\mathrm{T}}\boldsymbol{\xi}) - \boldsymbol{W}^{\mathrm{T}}\boldsymbol{\sigma}(\boldsymbol{V}^{\mathrm{T}}\boldsymbol{\xi}) = \tilde{\boldsymbol{W}}^{\mathrm{T}}(\hat{\boldsymbol{\sigma}} - \hat{\boldsymbol{\sigma}}'\hat{\boldsymbol{V}}^{\mathrm{T}}\boldsymbol{\xi}) + \hat{\boldsymbol{W}}^{\mathrm{T}}\hat{\boldsymbol{\sigma}}'\tilde{\boldsymbol{V}}^{\mathrm{T}}\boldsymbol{\xi} + \boldsymbol{d}, \tag{17}$$

where $\hat{\boldsymbol{\sigma}}' = \left.\dfrac{\mathrm{d}\boldsymbol{\sigma}}{\mathrm{d}z}\right|_{z=\hat{V}^{\mathrm{T}}\xi} = \begin{bmatrix} 0 & 0 & 0 \\ \sigma_1' & \cdots & 0 \\ \vdots & \ddots & \vdots \\ 0 & \cdots & \sigma_{N_2}' \end{bmatrix}$, and $\hat{\boldsymbol{\sigma}}' \in \Re^{(N_2+1)\times N_2}$ with

$$\sigma_r' = \sigma_r'(\sum_{k=1}^{N_1} \vartheta_{rk} x_k + \vartheta_{r(N_1+1)}) = \left.\frac{\mathrm{d}\sigma_r(\xi_r)}{\mathrm{d}\xi_r}\right|_{\xi_r = \sum_{k=1}^{N_1}\vartheta_{rk}x_k + \vartheta_{r(N_1+1)}}; \tag{18}$$

and the residual term $\boldsymbol{d}$ is given by

$$\boldsymbol{d} = \tilde{\boldsymbol{W}}^{\mathrm{T}}\hat{\boldsymbol{\sigma}}'\hat{\boldsymbol{V}}^{\mathrm{T}}\boldsymbol{\xi} - \boldsymbol{W}^{\mathrm{T}}O(\tilde{\boldsymbol{V}}^{\mathrm{T}}\boldsymbol{\xi})^2 = -\boldsymbol{W}^{\mathrm{T}}(\boldsymbol{\sigma} - \hat{\boldsymbol{\sigma}}) - \boldsymbol{W}^{\mathrm{T}}\hat{\boldsymbol{\sigma}}'\hat{\boldsymbol{V}}^{\mathrm{T}}\boldsymbol{\xi} + \hat{\boldsymbol{W}}^{\mathrm{T}}\hat{\boldsymbol{\sigma}}'\boldsymbol{V}^{\mathrm{T}}\boldsymbol{\xi}. \tag{19}$$

For the sigmoid activation function and $N_3 = 1$, we have

$$|\boldsymbol{d}| \le \|\boldsymbol{V}\|_F \left\|\boldsymbol{\xi}\hat{\boldsymbol{W}}^{\mathrm{T}}\hat{\boldsymbol{\sigma}}'\right\|_F + \|\boldsymbol{W}\|\left\|\hat{\boldsymbol{\sigma}}'\hat{\boldsymbol{V}}^{\mathrm{T}}\boldsymbol{\xi}\right\| + |\boldsymbol{W}|_1. \tag{20}$$

3. Target Tracking Design

The control design follows two steps. At first, a neural yaw controller is developed to stabilize the ψ_{ie} dynamics; then, a neural surge controller is designed to stabilize the z_{ie} dynamics by employing backstepping. The stability of the entire closed-loop system will be analyzed in subsection 3.3.

To move on, the following assumptions are needed:

Assumption 1: The disturbances $w_{iu}(t)$, $w_{i\upsilon}(t)$ and $w_{ir}(t)$ are bounded and there exist positive constants w_{iuM}, w_{ivM} and w_{irM} such that $|w_{iu}(t)| \le w_{iuM}$, $|w_{iv}(t)| \le w_{ivM}$, and $|w_{ir}(t)| \le w_{irM}$.

Definition 1: (Li *et al*., 2008)

Consider a system $\dot{x}_i = f(\boldsymbol{X}) + d_1$, where $\boldsymbol{X} = [x_1, ..., x_i, ..., x_n]^{\mathrm{T}}$, $f: \Re^n \to \Re$ is a function and d_1 is a disturbance term. For all bounded x_j, $j \ne i$ and d_1, if there exists a scalar function $V(x_i) \in C^1$ such that

a) $V(x_i)$ is globally positive definite and further radically unbounded;

b) $\dot{V}(x_i) < 0$ if $|x_i| > b$, where b is a positive constant and its magnitude is related to the bounds of x_j, $j \ne i$ and d_1; then, the variable x_i is passive-bounded.

Assumptions 2: Assume that the sway velocity υ_i is passive-bounded.

Remark 1: Passive-boundness of sway dynamics has been systematically analyzed by considering different cases in Li *et al*. (2008). This assumption is highly realistic since in practice the hydrodynamics damping force dominates in the sway direction and the sway speed is damped out by the force. Following Li *et al*. (2008), we make the same assumption on the sway dynamics.

3.1 Yaw Control

Taking the time derivative of ψ_{ie} twice and using Eqs. (5) and (8), we have

$$m_{33i}\ddot{\psi}_{ie}=m_{33i}\ddot{\psi}_{id}+m_{32i}m_{22i}^{-1}\left[c_{23i}(\nu_i)r_i+d_{22i}(\nu_i)\upsilon_i+d_{23i}(\nu_i)r_i+\Delta_v(\nu_i,\eta_i)\right]+c_{31i}(\nu_i)u_i+c_{32i}(\nu_i)\upsilon_i+d_{32i}(\nu_i)\upsilon_i+d_{33i}(\nu_i)r_i+\Delta_r(\nu_i,\eta_i)-\tau_{ir}-w_{i\varphi}, \tag{21}$$

where $w_{i\varphi}=m_{32i}m_{22i}^{-1}w_{i\upsilon}+w_{ir}$. Since $w_{i\upsilon}$ and w_{ir} are bounded, there exists a constant $w_{i\varphi M}$ such that $|w_{i\varphi}|\le w_{i\varphi M}$.

Introduce a filtered error state

$$\varphi_{ie}:=\dot{\psi}_{ie}+\lambda\psi_{ie}. \tag{22}$$

Then, the time derivative of Eq. (22) with Eq. (21) can be written as:

$$m_{33i}\dot{\varphi}_{ie}=f_{i1}(\cdot)-\tau_{ir}-w_{i\varphi}, \tag{23}$$

where

$$f_{i1}(\cdot)=m_{33i}\ddot{\psi}_{id}+m_{32i}m_{22i}^{-1}\left[c_{23i}(\nu_i)r_i+d_{22i}(\nu_i)\upsilon_i+d_{23i}(\nu_i)r_i+\Delta_v(\nu_i,\eta_i)\right]+c_{31i}(\nu_i)u_i+c_{32i}(\nu_i)\upsilon_i+d_{32i}(\nu_i)\upsilon_i+d_{33i}(\nu_i)r_i+\Delta_r(\nu_i,\eta_i)+m_{33i}\lambda\dot{\psi}_{ie}. \tag{24}$$

Note that $f_{i1}(\cdot)$ is an unknown function; thus, a SHL NN is used to approximate it as follows:

$$f_{i1}(\cdot)=\boldsymbol{W}_{i1}^{\mathrm{T}}\boldsymbol{\sigma}(\boldsymbol{V}_{i1}^{\mathrm{T}}\boldsymbol{\xi}_{i1})+\varepsilon_{i1}, \tag{25}$$

where $\boldsymbol{\xi}_{i1}=[\boldsymbol{\eta}_i^{\mathrm{T}},\boldsymbol{v}_i^{\mathrm{T}},\ddot{\psi}_{id},\dot{\psi}_{id},\psi_{id},1]^{\mathrm{T}}\in\Re^{10}$; ε_{i1} is a approximation error satisfying $\|\varepsilon_{i1}\|\le\varepsilon_{i1M}$ with ε_{i1M} a positive constant.

To cancel out the uncertain dynamics $f_{i1}(\cdot)$, an adaptive term, denoted by $\hat{f}_{i1}(\cdot)$, is introduced in the yaw control, which takes the form of

$$\hat{f}_{i1}(\cdot)=\hat{\boldsymbol{W}}_{i1}^{\mathrm{T}}\boldsymbol{\sigma}(\hat{\boldsymbol{V}}_{i1}^{\mathrm{T}}\boldsymbol{\xi}_{i1}). \tag{26}$$

Choose a yaw controller

$$\tau_{ir}=(k_{i1}+h_{i1})\varphi_{1e}+\hat{\boldsymbol{W}}_{i1}^{\mathrm{T}}\boldsymbol{\sigma}(\hat{\boldsymbol{V}}_{i1}^{\mathrm{T}}\boldsymbol{\xi}_{i1}) \tag{27}$$

with adaptive laws

$$\dot{\hat{\boldsymbol{W}}}_{i1}=\boldsymbol{\Gamma}_{\boldsymbol{W}_{i1}}[(\hat{\boldsymbol{\sigma}}-\hat{\boldsymbol{\sigma}}'\hat{\boldsymbol{V}}_{i1}^{\mathrm{T}}\boldsymbol{\xi}_{i1})\varphi_{ie}-k_{\boldsymbol{W}_{i1}}\hat{\boldsymbol{W}}_{i1}];$$

$$\dot{\hat{\boldsymbol{V}}}_{i1}=\boldsymbol{\Gamma}_{\boldsymbol{V}_{i1}}[\boldsymbol{\xi}_{i1}\varphi_{ie}\hat{\boldsymbol{W}}_{i1}^{\mathrm{T}}\hat{\boldsymbol{\sigma}}'-k_{\boldsymbol{V}_{i1}}\hat{\boldsymbol{V}}_{i1}]. \tag{28}$$

where $h_{i1}=k_{i4}\left(\left\|\boldsymbol{\xi}_{i1}\hat{\boldsymbol{W}}_{i1}^{\mathrm{T}}\hat{\boldsymbol{\sigma}}'\right\|_F^2+\left\|\hat{\boldsymbol{\sigma}}'\hat{\boldsymbol{V}}_{i1}^{\mathrm{T}}\boldsymbol{\xi}_{i1}\right\|^2+1\right)$, $\boldsymbol{\Gamma}_{\boldsymbol{W}_{i1}}>0, \boldsymbol{\Gamma}_{\boldsymbol{V}_{i1}}>0, k_{\boldsymbol{W}_{i1}}>0,$ and $k_{\boldsymbol{V}_{i1}}>0$.

Next, we are ready to get the closed-loop subsystem in the yaw direction. Substituting the control law Eq. (27) into Eq. (23) yields

$$m_{33i}\dot{\varphi}_{ie}=-\tilde{f}_{i1}(\cdot)-k_{i1}\varphi_{ie}-w_{i\varphi}, \tag{29}$$

where the function estimation error $\tilde{f}_{i1}(\cdot)$ is given by

$$\tilde{f}_{i1}(\cdot) = \hat{f}_{i1}(\cdot) - f_{i1}(\cdot) = \hat{\boldsymbol{W}}_{i1}^{\mathrm{T}}\boldsymbol{\sigma}(\hat{\boldsymbol{V}}_{i1}^{\mathrm{T}}\boldsymbol{\xi}_{i1}) - \boldsymbol{W}_{i1}^{\mathrm{T}}\boldsymbol{\sigma}(\boldsymbol{V}_{i1}^{\mathrm{T}}\boldsymbol{\xi}_{i1}) - \varepsilon_{i1}\,. \tag{30}$$

From Eq. (17), one can obtain

$$m_{33i}\dot{\varphi}_{ie} = -\tilde{\boldsymbol{W}}_{i1}^{\mathrm{T}}(\hat{\boldsymbol{\sigma}} - \hat{\boldsymbol{\sigma}}'\hat{\boldsymbol{V}}_{i1}^{\mathrm{T}}\boldsymbol{\xi}_{i1}) - \hat{\boldsymbol{W}}_{i1}^{\mathrm{T}}\hat{\boldsymbol{\sigma}}'\tilde{\boldsymbol{V}}_{i1}^{\mathrm{T}}\boldsymbol{\xi}_{i1} + \varepsilon_{i1} - d_{i1} - (k_{i1} + h_{i1})\varphi_{ie} - w_{i\varphi}\,, \tag{31}$$

where $\tilde{\boldsymbol{W}}_{i1} = \hat{\boldsymbol{W}}_{i1} - \boldsymbol{W}_{i1}$, and $\tilde{\boldsymbol{V}}_{i1} = \hat{\boldsymbol{V}}_{i1} - \boldsymbol{V}_{i1}$.

3.2 Surge Control

The surge controller is developed by employing the backstepping technique. At first, a virtual control α_{iu} is designed to stabilize z_{ie}. Next, the surge force τ_{iu} is designed to stabilize the surge dynamics.

Step I: Taking the time derivative of z_{ie} and recalling Eq. (10), we have

$$\dot{z}_{ie} = \dot{x}_{id}\cos\psi_{id} + \dot{y}_{id}\sin\psi_{id} + 2u_i\sin^2\tfrac{\psi_{ie}}{2} - u_i - \upsilon_i\sin\psi_{ie}\,. \tag{32}$$

Let $u_{ie} = \alpha_{iu} - u_i$, such that Eq. (32) becomes

$$\dot{z}_{ie} = \dot{x}_{id}\cos\psi_{id} + \dot{y}_{id}\sin\psi_{id} - \upsilon_i\sin\psi_{ie} + 2u_i\sin^2\frac{\psi_{ie}}{2} + u_{ie} - \alpha_{iu}\,. \tag{33}$$

To stabilize z_{ie}, choose a virtual control law

$$\alpha_{iu} = k_{i3}(z_{ie} - \delta_i) + \dot{x}_{id}\cos\psi_{id} + \dot{y}_{id}\sin\psi_{id} - \upsilon_i\sin\psi_{ie} + 2u_i\sin^2\frac{\psi_{ie}}{2}\,, \tag{34}$$

where $k_{i3} > 0$. $\delta_i > 0$ is used to avoid the sensitivity to calculate ψ_{id}. Similar approach can be found in Cui *et al*. (2010).

Consider a scalar positive function

$$L_{i1} = \frac{1}{2}\bar{z}_{ie}^2\,, \tag{35}$$

where $\bar{z}_{ie} = z_{ie} - \delta_i$. Taking the time derivative of L_{i1}, we have

$$\dot{L}_{i1} = \bar{z}_{ie}(\dot{x}_{id}\cos\psi_{id} + \dot{y}_{id}\sin\psi_{id} - \upsilon_i\sin\psi_{ie} + 2u_i\sin^2\frac{\psi_{ie}}{2} + u_{ie} - \alpha_{iu}) \tag{36}$$

It follows from Eq. (34) that $\dot{L}_{i1}$ can be written by

$$\dot{L}_{i1} = -k_{i3}\bar{z}_{ie}^2 + \bar{z}_{ie}u_{ie}\,. \tag{37}$$

Step II: Taking the time derivative of u_{ie}, we have

$$m_{11i}\dot{u}_{ie} = m_{11i}\dot{\alpha}_{iu} + c_{13i}(\nu_i)r_i + d_{11i}(\nu_i)u_i + \varDelta_u(\nu_i, \eta_i) - (\tau_{iu} + w_{iu})\,. \tag{38}$$

Consider another scalar positive function

$$L_{i2} = L_{i1} + \frac{1}{2}m_{11i}u_{ie}^2\,, \tag{39}$$

whose time derivative along Eq. (38) is

$$L_{i2} = -k_{i3}\bar{z}_{ie}^2 + u_{ie}[f_{i2}(\cdot) - (\tau_{iu} + w_{iu})]\,, \tag{40}$$

where $f_{i2}(\cdot) = m_{11i}\dot{\alpha}_{iu} + c_{13i}(\nu_i)r_i + d_{11i}(\nu_i)u_i + \varDelta_u(\nu_i, \eta_i) + \bar{z}_{ie}$.

As $f_{i2}(\cdot)$ is an unknown function, similarly, a SHL NN is used to approximate it as follows:

$$f_{i2}(\cdot)=\boldsymbol{W}_{i2}^{\mathrm{T}}\boldsymbol{\sigma}(\boldsymbol{V}_{i2}^{\mathrm{T}}\boldsymbol{\xi}_{i2})+\varepsilon_{i2}\,, \tag{41}$$

where $\boldsymbol{\xi}_{i2}=[\boldsymbol{\eta}_i^{\mathrm{T}},\boldsymbol{v}_i^{\mathrm{T}},\psi_{id},\bar{z}_{ie},\dot{\alpha}_{iu},1]^{\mathrm{T}}\in\Re^{10}$; ε_{i2} is an approximation error satisfying $\|\varepsilon_{i2}\|\le\varepsilon_{i2M}$ with ε_{i2M} a positive constant.

Similar to Eq. (26), an adaptive term $\hat{f}_{i2}(\cdot)$ is introduced to estimate the uncertain nonlinear dynamics $f_{i2}(\cdot)$, which takes the form of

$$\hat{f}_{i2}(\cdot)=\hat{\boldsymbol{W}}_{i2}^{\mathrm{T}}\boldsymbol{\sigma}(\hat{\boldsymbol{V}}_{i2}^{\mathrm{T}}\boldsymbol{\xi}_{i2})\,. \tag{42}$$

Now, select a surge controller as

$$\tau_{iu}=(k_{i2}+h_{i2})u_{ie}+\hat{\boldsymbol{W}}_{i2}^{\mathrm{T}}\boldsymbol{\sigma}(\hat{\boldsymbol{V}}_{i2}^{\mathrm{T}}\boldsymbol{\xi}_{i2}) \tag{43}$$

with adaptive laws

$$\dot{\hat{\boldsymbol{W}}}_{i2}=\varGamma_{W_{i2}}[(\hat{\boldsymbol{\sigma}}-\hat{\boldsymbol{\sigma}}'\hat{\boldsymbol{V}}_{i2}^{\mathrm{T}}\boldsymbol{\xi}_{i2})u_{ie}-k_{W_{i2}}\hat{\boldsymbol{W}}_{i2}];$$

$$\dot{\hat{\boldsymbol{V}}}_{i2}=\varGamma_{V_{i2}}[\boldsymbol{\xi}_{i2}u_{ie}\hat{\boldsymbol{W}}_{i2}^{\mathrm{T}}\hat{\boldsymbol{\sigma}}'-k_{V_{i2}}\hat{\boldsymbol{V}}_{i2}]. \tag{44}$$

where $h_{i2}=k_{i5}\left(\left\|\boldsymbol{\xi}_{i2}\hat{\boldsymbol{W}}_{i2}^{\mathrm{T}}\hat{\boldsymbol{\sigma}}'\right\|_F^2+\left\|\hat{\boldsymbol{\sigma}}'\hat{\boldsymbol{V}}_{i2}^{\mathrm{T}}\boldsymbol{\xi}_{i2}\right\|^2+1\right)$, $k_{i2}>0$, $\varGamma_{W_{i2}}>0$, $\varGamma_{V_{i2}}>0$, $k_{W_{i2}}>0$, and $k_{V_{i2}}>0$.

Substituting the control law Eq. (43) into Eq. (38), we get

$$m_{11i}\dot{u}_{ie}=\tilde{f}_{i2}(\cdot)-K_{i2}u_{ie}-w_{iu}\,, \tag{45}$$

where the function estimation error $\tilde{f}_{i2}(\cdot)$ satisfies

$$\tilde{f}_{i2}(\cdot)=\hat{f}_{i2}(\cdot)-f_{i2}(\cdot)=\hat{\boldsymbol{W}}_{i2}^{\mathrm{T}}\boldsymbol{\sigma}(\hat{\boldsymbol{V}}_{i2}^{\mathrm{T}}\boldsymbol{\xi}_{i2})-\boldsymbol{W}_{i2}^{\mathrm{T}}\boldsymbol{\sigma}(\boldsymbol{V}_{i2}^{\mathrm{T}}\boldsymbol{\xi}_{i2})-\varepsilon_{i2}\,. \tag{46}$$

Finally, recalling Eq. (17), we get the closed-loop surge subsystem

$$m_{33i}\dot{u}_{ie}=-\tilde{\boldsymbol{W}}_{i2}^{\mathrm{T}}(\hat{\boldsymbol{\sigma}}-\hat{\boldsymbol{\sigma}}'\hat{\boldsymbol{V}}_{i2}^{\mathrm{T}}\boldsymbol{\xi}_{i2})-\hat{\boldsymbol{W}}_{i2}^{\mathrm{T}}\hat{\boldsymbol{\sigma}}'\tilde{\boldsymbol{V}}_{i2}^{\mathrm{T}}\boldsymbol{\xi}_{i2}+\varepsilon_{i2}-d_{i2}-(k_{i2}+h_{i2})u_{ie}-w_{iu}\,, \tag{47}$$

where $\tilde{\boldsymbol{W}}_{i2}=\hat{\boldsymbol{W}}_{i2}-\boldsymbol{W}_{i2}$, and $\tilde{\boldsymbol{V}}_{i2}=\hat{\boldsymbol{V}}_{i2}-\boldsymbol{V}_{i2}$.

Remark 2: Li *et al*. (2008) considered the point tracking of marine craft. The key differences between our proposed control law and the control law in Li *et al*. (2008) are that: first, the vehicle kinetics in Li *et al*. (2008) only contains the linearly parameterized uncertainties, i.e, the uncertain parts of the kinetics are in the form of $\boldsymbol{\theta}^{\mathrm{T}}\boldsymbol{f}(\cdot)$ where $\boldsymbol{\theta}$ is an unknown vector and $\boldsymbol{f}(\cdot)$ is a vector composed of known functions. Therefore, the adaptive control law given in Li *et al*. (2008) cannot be applied to our case where the uncertain parts $f_{i1}(\cdot)$ and $f_{i2}(\cdot)$ are totally unknown; second, the singularity problem arising in the surge controller is avoided by our proposed control law.

3.3 Stability Analysis

By combining the above controller design for each subsystem, the main result of this paper is given as follow:

Theorem 1: Consider the leader-follower formation of N vehicles governed by the dynamics in Eqs. (1) and (2), and select the control laws in Eqs. (22) (27), (34) and (43) with adaptive laws in Eqs. (28) and (44) to track the virtual target in Eq. (9). If Assumptions 1 and 2 are satisfied, then all the signals in the closed-loop system are SUUB.

Proof: Construct the following Lyapunov function candidate

$$L = \frac{1}{2}\sum_{i=1}^{N}\{m_{33i}\varphi_{ie}^2 + \bar{z}_{ie}^2 + m_{11i}u_{ie}^2 + \sum_{j=1}^{2}[\tilde{\boldsymbol{W}}_{ij}^{\mathrm{T}}\Gamma_{W_{ij}}^{-1}\tilde{\boldsymbol{W}}_{ij} + \mathrm{tr}(\tilde{\boldsymbol{V}}_{ij}^{\mathrm{T}}\Gamma_{V_{ij}}^{-1}\tilde{\boldsymbol{V}}_{ij})]\}\,, \tag{48}$$

whose time derivative with Eqs. (31), (37) and (47) is given by

$$\begin{aligned}\dot{L} \le \sum_{i=1}^{N}\{&\varphi_{ie}[-\tilde{\boldsymbol{W}}_{i1}^{\mathrm{T}}(\hat{\boldsymbol{\sigma}} - \hat{\boldsymbol{\sigma}}'\hat{\boldsymbol{V}}_{i1}^{\mathrm{T}}\boldsymbol{\xi}_{i1}) - \hat{\boldsymbol{W}}_{i1}^{\mathrm{T}}\hat{\boldsymbol{\sigma}}'\tilde{\boldsymbol{V}}_{i1}^{\mathrm{T}}\boldsymbol{\xi}_{i1} + \varepsilon_{i1} - d_{i1} - (h_{i1} + k_{i1})\varphi_{ie} - w_{i\varphi}]\\ &-k_{i3}\bar{z}_{ie}^2 + u_{ie}[-\tilde{\boldsymbol{W}}_{i2}^{\mathrm{T}}(\hat{\boldsymbol{\sigma}} - \hat{\boldsymbol{\sigma}}'\hat{\boldsymbol{V}}_{i2}^{\mathrm{T}}\boldsymbol{\xi}_{i2}) - \hat{\boldsymbol{W}}_{i2}^{\mathrm{T}}\hat{\boldsymbol{\sigma}}'\tilde{\boldsymbol{V}}_{i2}^{\mathrm{T}}\boldsymbol{\xi}_{i2} + \varepsilon_{i2} - d_{i2} - (k_{i2} + h_{i2})u_{ie} - w_{iu}]\\ &+\sum_{j=1}^{2}[\tilde{\boldsymbol{W}}_{ij}^{\mathrm{T}}\Gamma_{W_{ij}}^{-1}\dot{\hat{\boldsymbol{W}}}_{ij} + \mathrm{tr}(\tilde{\boldsymbol{V}}_{ij}^{\mathrm{T}}\Gamma_{V_{ij}}^{-1}\dot{\hat{\boldsymbol{V}}}_{ij})]\}\,.\end{aligned} \tag{49}$$

Substituting Eqs. (28) and (44) into Eq. (49), we have

$$\begin{aligned}\dot{L} \le \sum_{i=1}^{N}\{&-(k_{i1} + h_{i1})\varphi_{ie}^2 + |\varphi_{ie}||d_{i1}| + |\varphi_{ie}|B_{i1M} - k_{i3}\bar{z}_{ie}^2 - (k_{i2} + h_{i2})u_{ie}^2\\ &+|u_{ie}||d_{i2}| + |u_{ie}|\mathrm{B}_{i2M} - \sum_{j=1}^{2}[k_{W_{ij}}\tilde{\boldsymbol{W}}_{ij}^{\mathrm{T}}\hat{\boldsymbol{W}}_{ij}^{\mathrm{T}} + k_{V_{ij}}\,\mathrm{tr}(\tilde{\boldsymbol{V}}_{ij}^{T}\hat{\boldsymbol{V}}_{ij})]\}\,,\end{aligned} \tag{50}$$

with $B_{i1M} \equiv \varepsilon_{i1M} + w_{i\varphi M}$ and $B_{i2M} \equiv \varepsilon_{i2M} + w_{iuM}$.

Using Young's inequality, the following inequalities hold

$$-k_{W_{ij}}\tilde{\boldsymbol{W}}_{ij}^{\mathrm{T}}\hat{\boldsymbol{W}}_{ij}^{\mathrm{T}} \le -\frac{k_{W_{ij}}}{2}\|\tilde{\boldsymbol{W}}_{ij}\|^2 + \frac{k_{W_{ij}}}{2}\|\boldsymbol{W}_{ij}\|^2, \quad j = 1, 2\,; \tag{51}$$

$$-k_{V_{ij}}\,\mathrm{tr}\{\tilde{\boldsymbol{V}}_{ij}^{\mathrm{T}}\hat{\boldsymbol{V}}_{ij}\} \le -\frac{k_{V_{ij}}}{2}\|\tilde{\boldsymbol{V}}_{ij}\|_F^2 + \frac{k_{V_{ij}}}{2}\|\boldsymbol{V}_{ij}\|_F^2, \quad j = 1, 2\,; \tag{52}$$

$$|\varphi_{ie}||d_{i1}| \le k_{i4}\|\varphi_{ie}\|^2\left(\|\boldsymbol{\xi}_{i1}\hat{\boldsymbol{W}}_{i1}^{\mathrm{T}}\hat{\boldsymbol{\sigma}}'\|_F^2 + \|\hat{\boldsymbol{\sigma}}'\hat{\boldsymbol{V}}_{i1}^{\mathrm{T}}\boldsymbol{\xi}_{i1}\|^2 + 1\right) + \frac{\|\boldsymbol{V}_{i1}\|_F^2 + \|\boldsymbol{W}_{i1}\|^2 + |\boldsymbol{W}_{i1}|_1^2}{4k_{i4}}\,; \tag{53}$$

$$|u_{ie}||d_{i2}| \le k_{i5}\|u_{ie}\|^2\left(\|\boldsymbol{\xi}_{i2}\hat{\boldsymbol{W}}_{i2}^{\mathrm{T}}\hat{\boldsymbol{\sigma}}'\|_F^2 + \|\hat{\boldsymbol{\sigma}}'\hat{\boldsymbol{V}}_{i2}^{\mathrm{T}}\boldsymbol{\xi}_{i2}\|^2 + 1\right) + \frac{\|\boldsymbol{V}_{i2}\|_F^2 + \|\boldsymbol{W}_{i1}\|^2 + |\boldsymbol{W}_{i2}|_1^2}{4k_{i5}}\,; \tag{54}$$

$$|\varphi_{ie}|\mathrm{B}_{i1M} \le k_{i6}\varphi_{ie}^2 + \frac{1}{4k_{i6}}\mathrm{B}_{i1M}^2\,; \ \ |u_{ie}|\mathrm{B}_{i2M} \le k_{i7}u_{ie}^2 + \frac{1}{4k_{i7}}\mathrm{B}_{i2M}^2\,. \tag{55}$$

Thus

$$\begin{aligned}\dot{L} &\le \sum_{i=1}^{N}\left\{-(k_{i1} - k_{i6})\varphi_{ie}^2 - \sum_{j=1}^{2}\left(\frac{k_{W_{ij}}}{2}\|\tilde{\boldsymbol{W}}_{ij}\|^2 + \frac{k_{V_{ij}}}{2}\|\tilde{\boldsymbol{V}}_{ij}\|_F^2\right) - k_{i3}\bar{z}_{ie}^2\right.\\ &\quad\left.-(k_{i2} - k_{i7})u_{ie}^2 + \left[\frac{k_{W_{ij}}}{2}\|\boldsymbol{W}_{ij}\|^2 + \frac{k_{V_{ij}}}{2}\|\boldsymbol{V}_{ij}\|_F^2 + \frac{\|\boldsymbol{V}_{ij}\|_F^2 + \|\boldsymbol{W}_{ij}\|^2 + |\boldsymbol{W}_{ij}|_1^2}{4k_{i(j+3)}} + \frac{B_{ijM}}{4k_{i(j+5)}}\right]\right\}\\ &\le -2\mu L + \varPhi\,,\end{aligned} \tag{56}$$

with

$$\mu := \min_{i=1,\ldots,N}\left\{k_{i1} - k_{i6},\, k_{i3},\, k_{i2} - k_{i7},\, \min_{j=1,2}\left[\frac{k_{W_{ij}}}{\lambda_{\max}(\Gamma_{W_{ij}}^{-1})}\right], \min_{j=1,2}\left[\frac{k_{V_{ij}}}{\lambda_{\max}(\Gamma_{V_{ij}}^{-1})}\right]\right\}; \tag{57}$$

$$\varPhi := \sum_{i=1}^{N}\left\{\sum_{j=1}^{2}\left[\frac{k_{W_{ij}}}{2}\|\boldsymbol{W}_{ij}\|^2 + \frac{k_{V_{ij}}}{2}\|\boldsymbol{V}_{ij}\|_F^2 + \frac{B_{ijM}}{4k_{i(j+5)}} + \frac{\|\boldsymbol{V}_{ij}\|_F^2 + \|\boldsymbol{W}_{ij}\|^2 + |\boldsymbol{W}_{ij}|^2}{4k_{i(j+3)}}\right]\right\}. \tag{58}$$

By integration of Eq. (56), it follows that

$$L(t) \le \frac{\Phi}{2\mu} + \left[L(0) - \frac{\Phi}{2\mu} \right] \exp(-2\mu t) \tag{59}$$

Note that L is bounded by $\frac{\Phi}{2\mu}$ as $t \to \infty$. Thus, the signals φ_{ie}, u_{ie}, $\bar{z}_{ie}$, $\tilde{\boldsymbol{W}}_{i1}$, $\tilde{\boldsymbol{V}}_{i1}$, $\tilde{\boldsymbol{W}}_{i2}$ and $\tilde{\boldsymbol{V}}_{i2}$ for $i = 1, ..., N$ are all SUUB. Since $\boldsymbol{W}_{i1}$, $\boldsymbol{V}_{i1}$, $\boldsymbol{W}_{i2}$ and $\boldsymbol{V}_{i2}$ are constants, we conclude that $\hat{\boldsymbol{W}}_{i1}$, $\hat{\boldsymbol{V}}_{i1}$, $\hat{\boldsymbol{W}}_{i2}$ and $\hat{\boldsymbol{V}}_{i2}$ are all SUUB. By Assumption 2, we know that υ_i is passive-bounded. Therefore, all signals in closed-loop system are SUUB. The proof is complete.

Remark 3: To improve the tracking performance, we provide the following design guidelines: (1) Increasing the number of the neurons will decrease the approximation bounds, which consequently results in a smaller tracking error. (2) From Eq. (57), it can be observed that the compact set to which the tracking errors converge can be deduced by increasing the control gains k_{i1}, k_{i2}, k_{i3}, $\Gamma_{W_{ij}}$ and $\Gamma_{V_{ij}}$.

4. Simulation

In this section, an example is given to illustrate the efficacy of the proposed control scheme. Referring to the nonlinear dynamical model of an experimental surface vessel used in Do and Pan (2006), the model parameters are given in Table 1.

Table 1 Model parameters

Parameter	Value	Parameter	Value
m_{11}	25.8	D_{11}	12+2.5|u|
m_{22}	33.8	D_{22}	17+4.5|υ|
m_{33}	2.76	D_{23}	0.2
m_{23}	6.2	D_{32}	0.5
m_{32}	6.2	D_{33}	0.5+0.1|r|

Without loss of generality, some uncertain dynamics and time-varying disturbances are introduced into the model, in particular,

$\Delta_i = [0.0112u^2\upsilon^3 + 0.0942\upsilon^2, 0.01u\upsilon r, 0.0257ur + 0.0793r^2\upsilon^2]^{\mathrm{T}}$;

$\boldsymbol{w}(t) = [0.254\cos(0.5t)\sin(0.2t) + 0.196\sin(0.3t)\cos(0.4t), 0.01\sin(0.2t), 0.05\sin(0.9t)\cos(0.2t)]^{\mathrm{T}}$.

In the formation setup, one vehicle is designated as the leader, another two as the followers. The formation is designed as $\boldsymbol{l}_{LF2} = [0, -2]^{\mathrm{T}}$ and $\boldsymbol{l}_{LF3} = [0, 2]^{\mathrm{T}}$. In the simulation, $\hat{\boldsymbol{W}}_1^{\mathrm{T}}\boldsymbol{\sigma}(\hat{\boldsymbol{V}}_1^{\mathrm{T}}\boldsymbol{\xi})$ and $\hat{\boldsymbol{W}}_2^{\mathrm{T}}\boldsymbol{\sigma}(\hat{\boldsymbol{V}}_2^{\mathrm{T}}\boldsymbol{\xi})$ contain eight neurons, respectively, and the activation function is selected as $1/\left[1+\exp(-x)\right]$. The control parameters for the control laws in Eqs. (22), (27), (34) and (43) with the adaptive laws in Eqs. (28) and (44) are chosen as follows: $\lambda = 2, k_{i1} = 10, k_{i2} = 1, k_{i3} = 10, \Gamma_{W_{i1}} = 100,$ $\Gamma_{W_{i2}} = 10,\ \Gamma_{V_{i1}} = 1, \Gamma_{V_{i2}} = 1,\ k_{W_{i1}} = k_{W_{i2}} = 0.3, k_{V_{i1}} = k_{V_{i2}} = 0.01$ and $k_{i4} = k_{i5} = 0.02.$

The path of the leader is generated as $x_{1d} = 10 - 10\cos(0.015t)$ and $y_{1d} = 10\sin(0.015t)$.

The simulation results are shown in Figs. 2~6. Fig. 2 shows the entire formation trajectories where the leader is commanded in a circular path. It can be observed that the formation is well established. The uncertainties in the surge and yaw direction and outputs of NNs are plotted in Figs. 3 and 4, where we note that the uncertainties in the model are efficiently compensated by the outputs of NNs. Fig. 5 demonstrates the boundedness of the control actions with respect to the two followers respectively, and no oscillation occurred during the adaptation process. Fig. 6 shows that with the proposed control law, the tracking errors converge to a very small neighborhood of the origin.

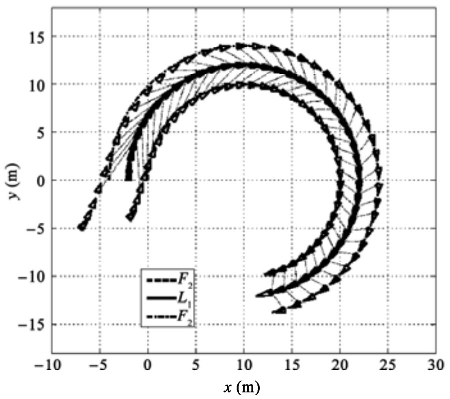

Fig. 2. Formation trajectories in 2-D plane.

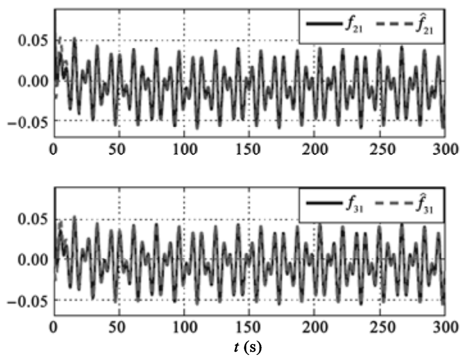

Fig. 3. NNs approximate the uncertainties in the yaw direction.

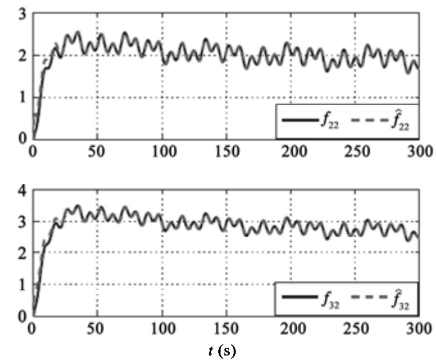

Fig. 4. NNs approximate the uncertainties in the surge direction.

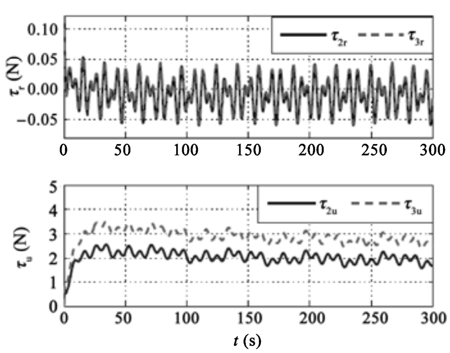

Fig. 5. Control efforts.

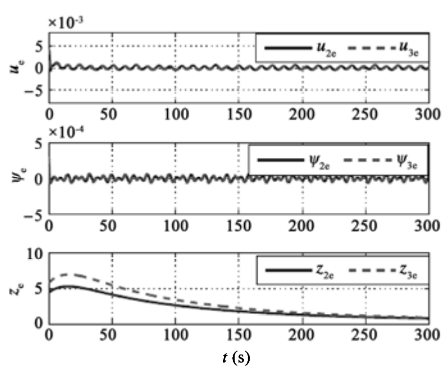

Fig. 6. Tracking errors.

5. Conclusions

This paper has presented the development of a neural formation controller for multiple marine surface vessels in the presence of unknown nonlinear dynamics caused by Coriolis/centripetal force, nonlinear damping, unmodeled hydrodynamics and unknown disturbances from the environment. Compared with the model-based control, the NN-based scheme shows some advantages to handle these uncertain dynamics. The stability of the closed-loop system has been proven by using Lyapunov theory. Simulation results have demonstrated the efficacy of the proposed method and the learning ability of NN.

Acknowledgments – The authors would like to give thanks to the editor and anonymous reviewers for their constructive comments and suggestions that have improved the quality of the paper.

References

Aguiar, A. P., Ghabcheloo, R., Pascoal, A., Silvestre, C., Hespanha, J. and Kaminer, I., 2006. Coordinated path-following of multiple underactuated autonomous vehicles with bidirectional communication constraints, *Proceedings of the 2nd International Symposium on Communications, Control and Signal Processing*, Morocco.

Aguiar, A., Almeida, J., Bayat, M., Cardeira, B., Cunha, R., Häusler, A., Maurya, P., Oliveira, A., Pascoal, A., Pereira, A., Rufino, M., Sebastião, L., Silvestre, C. and Vanni, F., 2009. Cooperative control of multiple marine vehicles: theoretical challenges and practical issues, *Proceedings of the MCMC09-8th Conference on Manoeuvring and Control of Marine Craft*, Guarujá , Brazil.

Almeida, J., Silvestre, C. and Pascoal, A., 2007. Coordinated control of multiple vehicles with discrete-time periodic communication, *Proceedings of the 46th IEEE Conference on Decision and Control*, 2888~2893.

Balch, T. and Arkin, R. C., 1999. Behavior-based formation control for multi-robot teams, *IEEE Transaction on Robotics and Automation*, **14**(6): 926~939.

Beard, R. W., Lawton, J. and Hadaegh, F. Y., 2001. A coordination architecture for spacecraft formation control, *IEEE Transaction on Control Systems Technology*, **9**(6): 777~790.

Børhaug, E., Pavlov, A., Ghabcheloo, R., Pettersen, K. Y., Pascoal, A. and Silvestre, C., 2006. Formation control of underactuated marine vehicles with communication constraints, *Proceedings of the 7th IFAC Conference on Maneuvering and Control of Marine Craft*.

Breivik, M., 2010. *Topics in Guided Motion Control of Marine Vehicles*, Ph. D. Thesis, Norwegian University of Science and Technology, 73~76.

Breivik, M., Hovstein, V. E. and Fossen, T. I., 2008a. Ship formation control: a guided leader-follower approach, *Proceedings of the 17th IFAC World Congress*, Seoul, Korea.

Breivik, M., Hovstein, V. E. and Fossen, T. I., 2008b. Straight-line target tracking for unmanned surface vehicles, *Modeling*, *Identification and Control*, 29(4): 131~149.

Chen, W. S., Jiao, L. C. and Wu, J. S., 2010. Globally stable adaptive robust tracking control using RBF neural networks as feedforward compensators, *Neural Computation and Application*, **21**(2): 351~363.

Chen, X. and Li, Y., 2008. Stability on adaptive NN formation control with variant formation patterns and interaction topologies, *Int. J. Adv. Robot. Syst.*, **5**(1): 69~82.

Cui, R. X., Ge, S. S., How, B. V. E. and Choo, Y. S., 2010. Leader-follower formation control of underactuated autonomous underwater vehicles, *Ocean Eng.*, **37**(17-18): 1491~1502.

Dierks, T. and Jagannathan, S., 2010. Neural network output feedback control of robot formations, *IEEE Transactions on Systems*, *Man*, *and Cybernetics*, *Part B*: *Cybernetics*, **40**(2): 383~399.

Do, K. D. and Pan, J., 2006. Global robust adaptive path following of underactuated ships, *Automatica*, **42**(10):

1713~1722.

Fahimi, F., 2006. Sliding mode formation control for under-actuated autonomous surface vehicle, *Proceedings of American Control Conference*, **33**(2): 4255~4260.

Fossen, T. I., 2002. *Marine Control System*: *Guidance*, *Navigation and Control of Ships*, *Rigs and Underwater Vehicles*, Trondheim, Norway, Marine Cybernetics.

Hornik, K., 1991. Approximation capabilities of multilayer feedforward networks, *Neural Network*, **4**(2): 251~257.

Hovakimyan, N., Nardi, F., Kim, N. and Calise, A. J., 2002. Adaptive output feedback control of uncertain systems using single hidden layer neural networks, *IEEE Transactions on Neural Networks*, **13**(6): 1420~1431.

Ihle, I.-A. F., Arcak, M. and Fossen, T. I., 2006. Passivity-based designs for synchronized path following, *Proceedings of the 45th IEEE Conference on Decision and Control*, 4319~4326.

Leonard, N. E. and Fiorelli, E., 2001. Virtual leader, artificial potentials and coordinated control of groups, *Proceedings of the 40th IEEE Conference on Decision and Control*, 2968~2973.

Lewis, F. L., Yesildirek, A. and Liu, K., 1996. Multilayer neural-net robot controller with guaranteed tracking performance, *IEEE Transactions on Neural Networks*, **7**(2): 388~399.

Li, J. H., Lee, P. M., Jun, B. H. and Lim, Y. K., 2008. Point-to-point navigation of underactuated ships, *Automatica*, **44**(12): 3201~3205.

Peng, Z. H., Wang, D. and Hu, X. J., 2011a. Robust adaptive formation control of underactuated autonomous surface vehicles with uncertain dynamics, *IET Control Theory and Applications*, **5**(12): 1378~1387.

Peng, Z. H., Wang, D., Chen, Z. Y., Hu, X. J. and Lan, W. Y., 2011b. Adaptive dynamic surface control of autonomous surface vehicles with uncertain dynamics, *IEEE Transaction on Control System Technology*, **99**, 1~8.

Polycarpou, M. M., 1996. Stable adaptive neural control scheme for nonlinear system, *IEEE Transactions on Automatic Control*, **41**(3): 447~451.

Skjetne, R., Moi, S. and Fossen, T. I., 2002. Nonlinear formation control of marine craft, *Proceedings of the 41st IEEE Conference on Decision and Control*, 1699~1704.

Tee, K. P. and Ge, S. S., 2007. Control of fully actuated ocean surface vessels using a class of feedforward approximators, *IEEE Transaction on Control System Technology*, **14**(4): 750~756.

Wang, D. and Huang, J., 2002. Adaptive neural network control for a class of uncertain nonlinear systems in pure-feedback form, *Automatica*, **38**(8): 1365~1372.

Wang, D. and Huang, J., 2005. Neural network based adaptive dynamic surface control for a class of uncertain nonlinear systems in strict-feedback form, *IEEE Transaction on Neural Networks*, **16**(1): 195~202.

Wang, D., 2010. Neural network-based adaptive dynamic surface control of uncertain nonlinear pure-feedback systems, *International Journal of Robust and Nonlinear Control*, **21**(5): 527~541.

Wang, P. K. C., 1991. Navigation strategies for multiple autonomous mobile robots moving in formation, *Journal of Robotic Systems*, **8**(2): 177~195.

Zhang, T., Ge, S. S. and Hang, C. C., 1999. Design and performance analysis of a direct adaptive controller for nonlinear systems, *Automatica*, **35**(11): 1809~1817.